Published in final edited form as:

JACC Cardiovasc Imaging. 2020 March ; 13(3): 790–801. doi:10.1016/j.jcmg.2019.06.015.

Intravascular Polarimetry in Patients With Coronary Artery Disease

Kenichiro Otsuka, MD, PhD[a], **Martin Villiger, PhD**[a], **Antonios Karanasos, MD, PhD**[b,c], **Laurens J.C. van Zandvoort, BSc**[b], **Pallavi Doradla, PhD**[a], **Jian Ren, PhD**[a], **Norman Lippok, PhD**[a], **Joost Daemen, MD, PhD**[b], **Roberto Diletti, MD, PhD**[b], **Robert-Jan van Geuns, MD, PhD**[b,d], **Felix Zijlstra, MD, PhD**[b], **Gijs van Soest, PhD**[b], **Jouke Dijkstra, PhD**[e], **Seemantini K. Nadkarni, PhD**[a], **Evelyn Regar, MD, PhD**[b,f], **Brett E. Bouma, PhD**[a,b,g]

[a]Wellman Center for Photomedicine, Massachusetts General Hospital, Harvard Medical School, Boston, MA USA; [b]Department of Cardiology, Thoraxcenter, Erasmus University Medical Center, Rotterdam, The Netherlands; [c]1st Department of Cardiology, Hippokration Hospital, University of Athens, Greece; [d]Department of Cardiology of Radboud UMC, Nijmegen, The Netherlands; [e]Division of Image Processing, Department of Radiology, Leiden University Medical Center, Leiden, The Netherlands; [f]Heart Center, University Hospital Zurich, Zurich, Switzerland; [g]Institute for Medical Engineering and Science, Massachusetts Institute of Technology, Cambridge, MA 02142, USA.

Abstract

Objectives: This first-in-human pilot study of intravascular polarimetry aimed to investigate polarization properties of coronary plaques in patients and to examine the relationship of these features with established structural characteristics available to conventional optical frequency domain imaging (OFDI) and with clinical presentation.

Background: Polarization-sensitive (PS-) OFDI measures birefringence and depolarization of tissue together with conventional cross-sectional OFDI images of subsurface microstructure.

Methods: 30 patients undergoing PS-OFDI (acute coronary syndrome; ACS, n=12 and stable angina pectoris; SAP, n=18) participated in this study. 342 cross-sectional images evenly distributed along all imaged coronary arteries were classified into one of seven plaque categories according to conventional OFDI. Polarization features averaged over the entire intimal area of each cross-section were compared between plaque types and with structural parameters. Further, we assessed the polarization properties in cross-sections (n=244) of the fibrous caps of ACS and SAP culprit lesions and compared them with structural features using a generalized linear model.

Results: The median birefringence and depolarization showed statistically significant differences among plaque types (both $p<0.001$, one-way ANOVA). Depolarization significantly differed

Address for Correspondence: Brett E. Bouma, Wellman Center for Photomedicine, Massachusetts General Hospital, Harvard Medical School, 50 Blossom Street, Boston, MA, 02114, Phone: +1-617-823-2619, Fax: +1-617-726-4103, bouma@mgh.harvard.edu.

Disclosures: Massachusetts General Hospital and the Erasmus University Medical Center have patent licensing arrangements with Terumo Corporation. Drs. Bouma, van Soest and Villiger have the right to receive royalties as part of the licensing arrangements. All other authors have reported that they have no relationships relevant to the contents of this paper to disclose.

between individual plaque types ($p<0.05$), except between normal arteries and fibrous plaques and between fibro-fatty and fibro-calcified plaques. Caps of ACS lesions and ruptured caps exhibited lower birefringence than caps of SAP lesions ($p<0.01$). In addition to clinical presentation, cap birefringence also associated with macrophage accumulation as assessed by normalized standard deviation.

Conclusions: Intravascular polarimetry provides quantitative metrics that help to characterize coronary arterial tissues and may offer refined insight into coronary arterial atherosclerotic lesions in patients.

Keywords

optical coherence tomography; atherosclerosis; collagen; inflammation; macrophage; polarized light

Introduction

Plaque morphology and composition have been implicated in the pathogenesis of acute coronary syndromes (ACS) (1, 2). The high resolution of optical coherence tomography (OCT) and optical frequency domain imaging (OFDI) has enabled identification of several structural features of plaque instability (3–6). Despite much progress, prospective identification of rupture-prone plaques, which would be crucial to stratify risk and improve patient management, remains elusive (7–10). Current OCT/OFDI imaging modalities rely on subjective interpretation and fall short of providing an objective and quantitative assessment of plaque morphology and composition (11–14).

Recently, we have introduced intravascular polarimetry by using polarization sensitive optical frequency domain imaging (PS-OFDI) in combination with standard intravascular OFDI catheters (15–17). Intravascular polarimetry complements the high resolution imaging of subsurface microstructures known from OCT and OFDI with polarimetric measurements of tissue birefringence and depolarization (15, 16). Tissue with fibrillar architecture, such as interstitial collagen or layered arrays of arterial smooth muscle cells, exhibits birefringence, which can serve to assess collagen and smooth muscle cell content (16, 18). Depolarization corresponds to the randomization of the detected polarization states (19) caused by the propagation of light through tissue containing lipid particles, macrophage accumulation, or cholesterol crystals (16). In our previous study comparing intravascular polarimetry with histopathology, we showed that tissue birefringence and depolarization provide useful compositional information and offer advanced tissue characterization (16). The present study aimed to investigate, for the first time, the polarization properties of atherosclerotic plaques in patients with coronary artery disease. We explored how the quantitative polarization metrics evaluated in entire cross-sections vary between different types of plaques, classified by conventional OFDI according to established qualitative structural criteria (plaque analysis). Moreover, we compared the polarization properties measured locally in the fibrous caps of culprit lesions between patients with ACS and SAP (cap analysis).

Methods

Study population

This first-in-human pilot study of intravascular polarimetry enrolled 30 non-consecutive patients (ACS, n = 12 and stable angina pectoris; SAP, n = 18) undergoing percutaneous coronary intervention at Erasmus University Medical Center (Erasmus MC) between December 2014 and July 2015. The ethics committee at Erasmus MC approved the protocol and each patient gave written informed consent before inclusion into the study, which was conducted in compliance with the protocol and the Declaration of Helsinki. PS-OFDI was performed using commercial intravascular catheters (FastView™, Terumo Corp., Tokyo, Japan) with a custom-built PS-OFDI system (Supplementary methods), as previously described (15–17). Imaging in the 30 patients yielded a total of 36 pullbacks, performed either before the procedure (n = 15, whereof culprit/target vessel, n = 13, and non-culprit/non-target vessel, n = 2) or after the procedure (n = 21). Patient characteristics are summarized in Table 1.

Study design

The present study comprises a plaque analysis evaluating entire cross-sections evenly distributed along all imaged coronary arteries and a cap analysis focusing solely on the fibrous cap of culprit lesions (Figure 1A). For the plaque analysis, all pullbacks were uniformly divided into segments of 5 mm length, progressing distally and proximally from the culprit lesion (Figure 1B). From the resulting total of 508 segments, comprising 2540 mm pullback length, 166 segments were excluded from the analysis due to the following criteria: 1) containing a stent or from within 5 mm proximal or distal to an implanted stent (n = 150); 2) subject to pre-dilatation (n = 2); and, 3) poor image quality due to insufficient blood clearing (n = 14). In each of the retained 342 5 mm-segments, only the cross section with the smallest lumen area was identified for further analysis. If this cross-section contained a side branch of diameter > 1.5 mm it was replaced with another section from the same segment. For segments containing fibroatheromas, instead of the smallest lumen area, the cross-section with the thinnest fibrous cap thickness was used for analysis.

For the cap analysis, we identified the culprit lesion in patients with ACS (n = 4) and SAP (n = 9) who underwent PS-OFDI imaging prior to percutaneous coronary intervention (Figure 1A). ACS culprit lesions were identified based on invasive coronary angiography, electrocardiographic ST-segment alterations, and/or regional wall motion abnormality on echocardiographic assessment. SAP target lesions were determined on the basis of left ventricular wall motion abnormalities, nuclear scan, stress test, and coronary angiographic findings. For the cap analysis, we identified the cross section with the smallest luminal area in the culprit/target lesion of each patient (Figure 1B). Every other cross-sectional image up to 5 mm both proximally and distally, if featuring a lipid arc exceeding > 90 degree, was included into the analysis, resulting in a total of 244 cross-sections.

Conventional OFDI analysis

Two independent investigators (A.K. and L.Z.) analyzed the conventional OFDI appearance of the selected images using QCU-CMS viewing software (Leiden University Medical

Center, Leiden, The Netherlands). Conventional OFDI analysis was performed blinded to the polarimetric signals. Luminal area was measured in all cross-sections. Percent area stenosis was calculated as previously reported (8), taking the mean of the largest lumen within 5 mm proximal and distal to the lesion containing the current cross-section as the reference.

Each selected cross-section was then categorized as either of normal artery, fibrous plaque (FP), fibro-fatty plaque (FF), fibro-calcified plaque (FC), thick cap fibroatheroma (ThCFA), thin cap fibroatheroma (TCFA), or plaque rupture (PR), based on the conventional OFDI signal (Figure 2 A1 to G1). Briefly, a vessel with a tunica intima thinner or similar in thickness to the tunica media was labelled as normal artery (Figure 2 A1). FP was defined asa plaque with high backscattering and relatively homogeneous OFDI signal (Figure 2 B1). Plaques with calcium, that appears as signal-poor or heterogeneous region with a sharply delineated border within fibrous tissue, were classified as FC (Figure 2 D1) (9). A plaque with a lipid arc of more than 90 degrees was defined as a fibroatheroma. A lipid-rich plaque with a lipid arc extending less than 90 degrees was categorized as FF, to appreciate the optical properties of the small lipid-rich area (Figure 2 C1). In fibroatheromas, the fibrous cap thickness was measured around its thinnest part 3 times by each observer and then the averaged value was calculated. If the fibrous cap thickness was <65 μm the plaque was categorized as TCFA and as ThCFA otherwise. PR was defined as a plaque featuring intimal disruption and cavity formation (Figure 2 E1 to G1). In cases of discordance between the observers, a third investigator (B.B.) acted as referee to achieve consensus classification and the majority was used as the final plaque classification.

Quantitative birefringence and depolarization analysis

PS-OFDI analysis was performed at Massachusetts General Hospital blinded to the conventional OFDI measurements and clinical information. Co-registration between conventional OFDI and polarimetric signals is intrinsic, since they are computed from the exact same raw data. For the plaque analysis, we segmented the intimal layer of each cross section using custom-written software in MATLAB (The MathWorks, Inc., Natick, Massachusetts). In addition to the lumen, we segmented the internal elastic lamina (IEL), whenever visible, using the birefringence map to leverage from the improved visibility of the media in the birefringence map (16). In areas where the IEL segmentation was unattainable, typically in lipid-rich areas of advanced lesions, an automatic outer border corresponding to a tissue depth of 1 mm from the lumen surface was used. We also segmented calcifications and areas of thrombus. To compute the average birefringence of cross-sections, we evaluated the median of the birefringence in the area bounded by the lumen and the IEL or outer border segmentation, excluding the guidewire shadow, and featuring a depolarization of ≤0.2 as previously reported (17). The median depolarization was computed within the entire segmented area after masking the guidewire shadow.

For the cap analysis, the border between the fibrous caps of the culprit fibroatheromas and the underlying lipid/necrotic core was drawn manually, together with the lipid arc angle extending from the center of the lumen (total cap analysis). Mean and thinnest fibrous cap thickness were automatically calculated from the segmented fibrous cap in MATLAB.

Furthermore, to investigate the features of fibrous caps at their thinnest part (focal cap analysis), we also defined a narrower arc angle, centered on the thinnest part of each cap (29˚ on average). In addition, we evaluated the normalized standard deviation (NSD) within the fibrous caps, which has been shown to correlate with macrophage infiltration (3, 12). NSD was computed by first evaluating the standard deviation of the linear-scale backscatter intensity data within elliptical regions of interest, extending by 80 μm in depth and 12˚ in the circumferential direction and moved across the entire cap area. These values were then normalized with the difference between the maximum and the minimum intensity within each fibrous cap.

Statistical analysis

Continuous outcome measures were reported as mean ± SD. For the plaque analysis, the mean of the birefringence and of the logarithm of the depolarization values across the different plaque types were compared with one-way analysis of variance. Pairwise comparison was performed with the Bonferroni correction if the overall test was significant. For comparison with clinical presentation in the cap analysis, the one PR lesion in the SAP group was classified together with the ACS lesions into an ACS and/or PR group. Differences in the means between the two groups were analyzed with a univariate generalized linear model using a generalized estimating equation to take into consideration the intra-subject correlations among multiple cross-sectional images from individual patients. The relationship between polarization properties and clinical and conventional OFDI parameters were determined by a univariate generalized linear model using a generalized estimating equation. β and 95% confidence interval (CI) for birefringence are given in units of $\times 10^{-3}$ throughout the manuscript. A p-value of <0.05 was considered to indicate statistical significance, and all tests were two-sided. SPSS 22.0 was used for all analyses (IBM Corp., Armonk, NY, USA).

Results

Polarization properties of individual plaque types

Table 1 summarizes patient characteristics and OFDI parameters for the overall study population. The selected 342 cross-sectional images representing all imaged vessels were classified into normal artery (n = 31), FP (n = 84), FF (n = 45), FC (n = 81), ThCFA (n = 88), TCFA (n = 11), and plaque rupture (n = 2) based on conventional OFDI. Computing the weighted κ coefficient for multiple categories, excellent intra and interobserver agreement was observed for the seven plaque categories (κ = 0.98 and κ = 0.97, respectively). Figure 3 shows significant differences in median birefringence and depolarization among the 7 plaque types (p < 0.001 for both, One-way ANOVA). Comparing individual plaque types, normal arteries were significantly less birefringent than all other plaque types (p < 0.01), except for TCFA (p = 0.124) and PR (p = 1.00). FPs featured the highest birefringence, followed by FFs, FCs, ThCFAs, TCFAs and PRs in decreasing order, but without statistical significance between individual categories (Figure 3A). Normal arteries also featured the lowest depolarization. Plaque rupture showed the highest depolarization among the 7 plaque types. Except FF versus FC, ThCFA versus TCFA, ThCFA versus PR, and TCFA versus PR, all

plaque types had statistically significant differences in depolarization when compared individually (Figure 3B).

Calcifications featured low birefringence and low depolarization (Supplementary Figure S1 A and B). Calcifications located in fibrous tissue exhibited lower birefringence and depolarization than those in lipid-rich lesions (both $p < 0.001$), as shown in Supplementary Figure S1 C and D. Thrombus (white thrombus) presented very low birefringence and depolarization (Supplementary Figure S2 A and B).

Polarization properties of fibrous caps in culprit lesions

The lipid arc and minimum fibrous cap thickness differed with statistical significance between the ACS/PR and the SAP group, as shown in Table 2. When comparing the polarimetric signals of the fibrous caps in the culprit lesions we found a lower birefringence in the ACS/PR group than in SAP patients ($p = 0.002$), but comparable depolarization ($p = 0.772$) (Figure 4A and B).

Table 3 shows generalized estimating equation model parameters for the relationship between polarization properties, clinical presentation, and conventional OFDI parameters, when analyzing the entire cap. Birefringence of the total cap was negatively correlated with ACS/PR ($\beta = -0.156$; $p = 0.002$) and NSD ($\beta = -0.021$; $p = 0.013$). Depolarization of the total cap was negatively associated with mean fibrous cap thickness ($\beta = -0.001$; $p < 0.001$) and positively with lipid arc ($\beta = 0.001$; $p = 0.001$) and tended to be correlated with NSD ($\beta = 0.005$; $p = 0.062$). Further, we analyzed narrow regions of interest centered on the thinnest part of each fibrous cap (Table 4). The generalized linear model using generalized estimating equation showed that ACS/PR ($\beta = -0.138$; $p < 0.001$), thinnest fibrous cap thickness ($\beta = 0.005$; $p = 0.001$) and NSD ($\beta = -0.012$; $p = 0.001$) were associated with birefringence. Factors associated with depolarization were thinnest fibrous cap thickness ($\beta = -0.001$; $p = 0.005$) and NSD ($\beta = 0.004$; $p < 0.001$).

Discussion

This first-in-human pilot study of intravascular polarimetry demonstrates how it augments conventional OFDI plaque characterization with quantitative polarization properties, measured through standard intravascular OFDI catheters simultaneously with the conventional OFDI signal. The polarization features offer refined insight into tissue composition, consistent with our current understanding of the mechanisms involved in plaque progression and destabilization. The major finding of this study is that fibrous caps in ACS culprit lesions and ruptured plaques exhibit lower birefringence compared to the caps of target lesions in SAP patients within our limited study cohort. Compared to the interpretation of conventional OFDI, which relies on subjective identification of qualitative features, polarimetry offers quantitative metrics, leading a way to objective and automated characterization of atherosclerotic plaques, which may facilitate the use of intravascular imaging in clinical practice. The improved assessment of plaque composition afforded by the polarization features may provide novel insight into the mechanism of plaque progression and instability in human coronary atherosclerosis.

Polarimetric plaque characterization

Smooth muscle cells and collagen are known to influence the polarization of near infrared light (18). Our recent study of intravascular PS-OFDI in cadaveric human hearts revealed that normal intimal tissue exhibits low birefringence compared to intimal tissue in fibrous, early, and advanced atherosclerotic lesions (16). In the present study, we observed significant differences in polarization properties, especially in depolarization, among all plaque types, despite analyzing the entire manually segmented intimal layer, comprising both the angle subtended by the plaque and the remainder of the cross-section. Depolarization featured significant differences even between individual plaque types, whereas birefringence was less distinguishing. These observations suggest that PS-OFDI provides insight into biological aspects of plaque progression and destabilization, complementary to the structural information available to conventional OFDI. Combined analysis of birefringence and depolarization in more refined automatically segmented regions of interest may offer automated tissue characterization. Moreover, accurate diagnosis of TCFA by OCT/OFDI remains challenging (13), and future studies are warranted to investigate the polarization features of thin and thick fibrous caps and early and late necrotic cores in detail.

Polarization properties in fibrous caps

Within our limited patient cohort, we observed that the fibrous cap of the culprit lesion in ACS/PR patients exhibited significantly lower birefringence than in the caps of target lesions in SAP patients. Fibrillar collagen is the primary extracellular matrix molecule imparting both birefringence and mechanical stability to the fibrous cap overlying an atheroma (20). Histopathological studies showed that ruptured fibrous caps lack layered smooth muscle cells and feature different collagen phenotypes than intact caps (20), which offers an explanation for the low birefringence observed in the fibrous caps of ACS/PR patients. In addition to cap birefringence, minimum fibrous cap thickness and lipid arc angle also featured statistically significant differences between these two patient groups. Yet, fibrous cap thickness alone is insufficient to identify caps that are prone to rupture (4, 5, 8, 9). The polarization metrics available to intravascular polarimetry complement these structural features and may advance our understanding of the pathogenesis of ACS with or without fibrous cap rupture (10, 21).

Furthermore, birefringence and depolarization of the fibrous cap were associated with increased NSD, suggesting macrophage accumulation. Inflammation is a known mechanism of plaque destabilization (2, 22, 23). Macrophages release enzymes including matrix metalloproteinases that destroy the extracellular matrix and weaken the cap (22). Our observations suggest that the presence of active macrophages may increase depolarization, whereas the effect of their presence causes a reduction in birefringence. The physical mechanism inducing depolarization in atherosclerosis remains to be elucidated. We speculate that lipid droplets exceeding the size of the wavelength used for OFDI and small cholesterol crystals, which have been postulated to be a crucial factor in the initiation of inflammatory response in atherosclerosis (24), are the origin of the observed depolarization.

Consistent with our previous cadaveric human heart study of intravascular polarimetry (16), we observed that calcifications located in fibrous tissue exhibited lower birefringence and depolarization than those in lipid-rich lesions. Although the OFDI appearance of microcalcifications has not been established (6), we speculate that their presence in fibrous caps contributes to a reduction of the cap birefringence, together with a lack of collagen organization and content and absence of SMCs. The few occurrences of white thrombus in the present study had minimal impact on the underlying polarization signatures. However, the stronger attenuation of red thrombus may lead to an apparent increase in depolarization that would impair interpretation of the underlying vessel wall, similar to conventional OFDI imaging.

Study limitations

First, our study consists of a small number of patients from a cohort of nonconsecutive patients and was cross-sectional in design. Considering potential selection bias of patients, our findings should be interpreted with caution, although we included all patients imaged with intravascular polarimetry. Furthermore, the limited number may lead to a potential over estimation of the differences between polarization features when performing multiple pairwise comparisons and prevented multivariate analysis. Owing to its compatibility with clinical OFDI imaging catheters, intravascular polarimetry can be readily applied to any patient eligible for conventional OFDI imaging, and future well-designed studies are needed to ascertain our current findings. Second, our plaque classification corresponds well to the current understanding of plaque subtypes in OFDI (6) and could be readily performed on the conventional OFDI signal, yet conventional OFDI has limited ability to classify lesion types, especially in advanced lesions (11, 14). Although lipid-rich plaques offer some prognostic implication (8), clear identification of fibroatheromas with OCT/OFDI remains debatable. Combination of intravascular ultrasound and OCT/OFDI has been shown to improve diagnostic accuracy of identifying fibroatheromas (13). Future histopathological validation studies are needed to inspect the ability of polarization properties to distinguish between different plaque types and potentially enable automated plaque classification. Third, we observed that NSD was associated with depolarization in the focal fibrous caps but not in the entire caps. Macrophage infiltration frequently occurs very locally and averaging the signals across entire caps carries less meaning than across a local region of interest. Moreover, the required normalization of the NSD depends delicately on the ROI, and evidence supporting the NSD metric remains scant. We suspect that both NSD and depolarization capture aspects of macrophage infiltration, but validation studies with histology are needed to identify how depolarization relates to macrophage infiltration. Finally, no patient in the current study presented plaque erosion, the second most common cause of ACS.

Conclusions

This study presents polarization properties of coronary atherosclerotic lesions in patients with coronary artery disease. The fibrous caps of culprit lesions in ACS/PR patients featured lower birefringence than in SAP patients. When averaged across entire cross-sections, the polarimetric signals varied among distinct morphological plaque subtypes. Quantitative assessment of plaque polarization properties by intravascular polarimetry may open new

avenues for studying plaque composition and detecting high-risk patients. Prospective studies in larger populations are needed to evaluate how polarization metrics could translate into improved patient outcomes and optimized medical therapy compared to utilizing only the structural features available to conventional OFDI.

Competencies in Medical Knowledge

Modification of the optical frequency domain imaging (OFDI) apparatus along with recently developed image reconstruction methods enabled measurements of polarization properties of the coronary arterial wall. Intravascular polarimetry permits quantitative assessment of polarization properties through standard intravascular OFDI catheters simultaneously with intensity image cross-sections. This first-in-human pilot study of intravascular polarimetry demonstrated that polarization properties differ between culprit lesions of acute coronary syndrome or plaque rupture and stable angina pectoris, and also among different morphological plaque subtypes.

Translational Outlook

Quantitative assessment of plaque structure and composition by intravascular polarimetry may open new avenues for studying coronary atherosclerosis and may facilitate the automated interpretation of lesion characteristics during percutaneous coronary intervention in patients. Future studies are needed to investigate how intravascular polarimetry may improve invasive and pharmacological interventions in patients with coronary artery disease.

Supplementary Material

Refer to Web version on PubMed Central for supplementary material.

Acknowledgements:

The authors sincerely thank Dr. Peter Libby of Brigham and Women’s Hospital and Harvard Medical School for fruitful discussion and feedback on this manuscript. Dr. Hang Lee, Biostatistics Center, Massachusetts General Hospital, Harvard Medical School, provided invaluable guidance with respect to the statistical analyses of this work. Dr. Otsuka acknowledges partial support from the Japan Heart Foundation/Bayer Yakuhin Research Grant Abroad, the Uehara Memorial Foundation Postdoctoral Fellowship, and the Japan Society for the Promotion of Science Overseas Research Fellowship.

Funding: This work was supported by the National Institutes of Health (grants P41EB-015903 and R01HL-119065) and by Terumo Corporation. Dr. Bouma was supported in part by the Professor Andries Querido visiting professorship of the Erasmus University Medical Center in Rotterdam.

Abbreviations

ACS	acute coronary syndrome
FC	fibro-calcified plaque
FF	fibro-fatty plaque
FP	fibrous plaque
NSD	normalized standard deviation

OCT	optical coherence tomography
OFDI	optical frequency domain imaging
PR	plaque rupture
PS-OFDI	polarization-sensitive optical frequency domain imaging
SAP	stable angina pectoris
TCFA	thin cap fibroatheroma
ThCFA	thick cap fibroatheroma

References

1. Virmani R, Burke AP, Farb A, Kolodgie FD. Review 2006 pathology of coronary vulnerable plaque. J Am Coll Cardiol 2006;47:C13–8. [PubMed: 16631505]
2. Narula J, Nakano M, Virmani R, et al. Histopathologic characteristics of atherosclerotic coronary disease and implications of the findings for the invasive and noninvasive detection of vulnerable plaques. J Am Coll Cardiol 2013;61:1041–1051. [PubMed: 23473409]
3. Tearney GJ, Yabushita H, Houser SL, et al. Quantification of macrophage content in atherosclerotic plaques by optical coherence tomography. Circulation 2003;107:113–119. [PubMed: 12515752]
4. Toutouzas K, Karanasos A, Tsiamis E, et al. New insights by optical coherence tomography into the differences and similarities of culprit ruptured plaque morphology in non-ST-elevation myocardial infarction and ST-elevation myocardial infarction. Am Heart J 2011;161:1192–1199. [PubMed: 21641368]
5. Yonetsu T, Kakuta T, Lee T, et al. In vivo critical fibrous cap thickness for rupture-prone coronary plaques assessed by optical coherence tomography. Euro Heart J 2011;32:1251–1259.
6. Tearney GJ, Regar E, Akasaka T, et al. Consensus standards for acquisition, measurement, and reporting of intravascular optical coherence tomography studies: A report from the International Working Group for Intravascular Optical Coherence Tomography Standardization and Validation. J Am Coll Cardiol 2012;59:1058–1072. [PubMed: 22421299]
7. Arbab-Zadeh A, Fuster V. The myth of the “vulnerable plaque”: Transitioning from a focus on individual lesions to atherosclerotic disease burden for coronary artery disease risk assessment. J Am Coll Cardiol 2015;65:846–855. [PubMed: 25601032]
8. Xing L, Higuma T, Wang Z, et al. Clinical Significance of Lipid-Rich Plaque Detected by Optical Coherence Tomography: A 4-Year Follow-Up Study. J Am Coll Cardiol 2017;69:2502–2513. [PubMed: 28521888]
9. Zhang BC, Karanasos A, Gnanadesigan M, et al. Qualitative and quantitative evaluation of dynamic changes in non-culprit coronary atherosclerotic lesion morphology: A longitudinal OCT study. EuroIntervention 2018;13:e2190–e2200. [PubMed: 29131800]
10. Garcia-Garcia HM, Jang IK, Serruys PW, Kovacic JC, Narula J, Fayad ZA. Imaging plaques to predict and better manage patients with acute coronary events. Circ Res 2014;114:1904–1917. [PubMed: 24902974]
11. Manfrini O, Mont E, Leone O, et al. Sources of error and interpretation of plaque morphology by optical coherence tomography. Am J Cardiol 2006;98:156–159. [PubMed: 16828584]
12. Phipps JE, Vela D, Hoyt T, et al. Macrophages and intravascular OCT bright spots: A quantitative study. J Am Coll Cardiol Img 2015;8:63–72.
13. Nakano M, Yahagi K, Yamamoto H, et al. Additive Value of Integrated Backscatter IVUS for Detection of Vulnerable Plaque by Optical Frequency Domain Imaging: An Ex Vivo Autopsy Study of Human Coronary Arteries. J Am Coll Cardiol Img 2016;9:163–172.

14. Phipps JE, Hoyt T, Vela D, et al. Diagnosis of Thin-Capped Fibroatheromas in Intravascular Optical Coherence Tomography Images: Effects of Light Scattering. Circ Cardiovasc interventions 2016;9.
15. van der Sijde JN, Karanasos A, Villiger M, Bouma BE, Regar E. First-in-man assessment of plaque rupture by polarization-sensitive optical frequency domain imaging in vivo. Euro Heart J 2016;37:1932.
16. Villiger M, Otsuka K, Karanasos A, et al. Coronary Plaque Microstructure and Composition Modify Optical Polarization. A New Endogenous Contrast Mechanism for Optical Frequency Domain Imaging. J Am Coll Cardiol Img 2018;11:1666–1676.
17. Villiger M, Otsuka K, Karanasos A, et al. Repeatability Assessment of Intravascular Polarimetry in Patients. IEEE Transactions on Medical Imaging 2018;37:1618–1625. [PubMed: 29969412]
18. Nadkarni SK, Pierce MC, Park BH, et al. Measurement of Collagen and Smooth Muscle Cell Content in Atherosclerotic Plaques Using Polarization-Sensitive Optical Coherence Tomography. J Am Coll Cardiol 2007;49:1474–1481. [PubMed: 17397678]
19. Lippok N, Villiger M, Albanese A, et al. Depolarization signatures map gold nanorods within biological tissue. Nature Photonics 2017;11:583–588. [PubMed: 29201136]
20. Yahagi K, Kolodgie FD, Otsuka F, et al. Pathophysiology of native coronary, vein graft, and in-stent atherosclerosis. Nat Rev Cardiol 2016;13:79–98. [PubMed: 26503410]
21. Niccoli G, Montone RA, Di Vito L, et al. Plaque rupture and intact fibrous cap assessed by optical coherence tomography portend different outcomes in patients with acute coronary syndrome. Euro Heart J 2015;36:1377–1384.
22. Galis ZS, Sukhova GK, Lark MW, Libby P. Increased expression of matrix metalloproteinases and matrix degrading activity in vulnerable regions of human atherosclerotic plaques. J Clin Invest 1994;94:2493–2503. [PubMed: 7989608]
23. Ridker PM, Everett BM, Thuren T, et al. Antiinflammatory Therapy with Canakinumab for Atherosclerotic Disease. N Engl J Med 2017:NEJMoa1707914.
24. Duewell P, Kono H, Rayner KJ, et al. NLRP3 inflammasomes are required for atherogenesis and activated by cholesterol crystals. Nature 2010;464:1357–1361. [PubMed: 20428172]

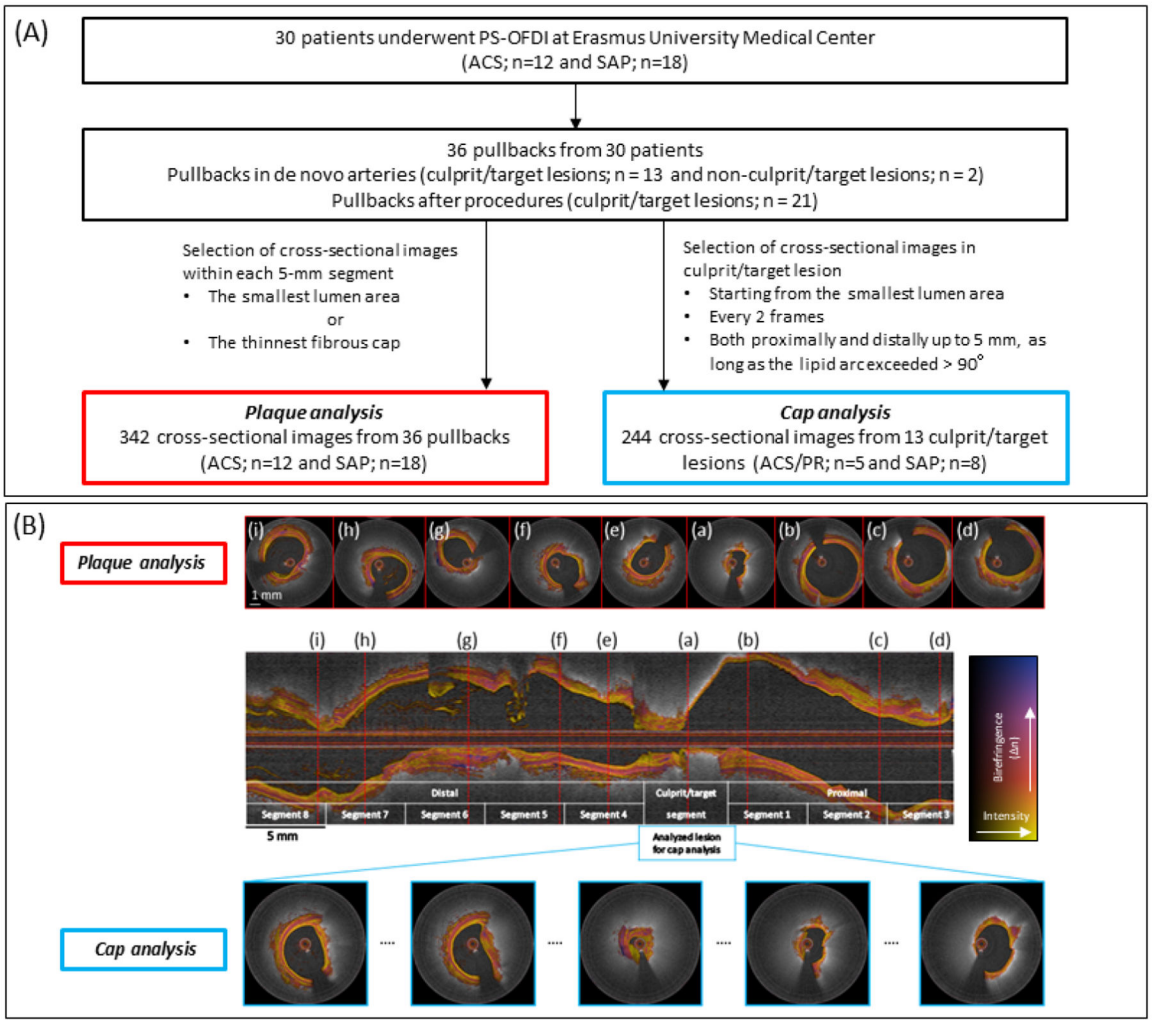

Figure 1. Study population, design and lesion selection

(A) Study population and data analysis. **(B)** PS-OFDI pullbacks were divided into 5 mm segments, centered on the culprit segment for the plaque analysis. Red broken lines indicate the selected cross-sectional images within each 5 mm segment, corresponding to the cross-section with the smallest luminal area. The cap analysis focused on the culprit/target segment centered around the cross section with the smallest luminal area in the culprit lesion of each patient. Cross-sectional images were analyzed every 2 frames both proximally and distally up to 5 mm, as long as the lipid arc exceeded > 90 degrees. Scale bars measure 1 mm for cross-sectional images (white) and 5 mm for the longitudinal image (black), respectively. ACS = acute coronary syndrome, PR = plaque rupture, SAP = stable angina pectoris, and PS-OFDI = polarization-sensitive optical frequency domain imaging.

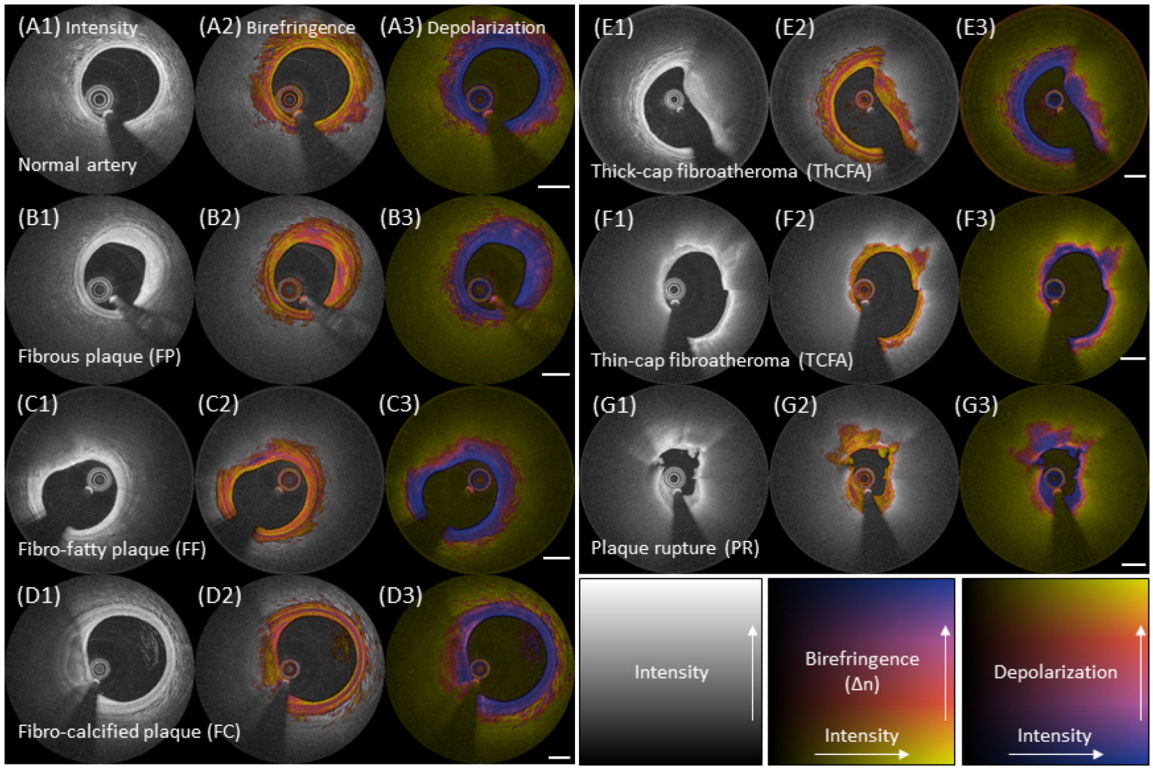

Figure 2. Representative PS-OFDI for all plaque types

(A1 to G1) Typical intensity images, **(A2 to G2)** birefringence images, and **(A3 to G3**) depolarization images of all plaque types. Rows show representative images of normal artery **(A1 to A3)**, FP **(B1 to B3)**, FF **(C1 to C3)**, FC **(D1 to D3)**, ThCFA **(E1 to E3)**, TCFA **(F1 to F3)**, and PR **(G1 to G3)**, respectively. **(A2 and A3)** Normal artery feature very low birefringence and low depolarization in the intima. The media features high birefringence, independent of the lesion type, and is clearly visible in normal arteries. **(B2 and B3)** Fibrous tissue in FP exhibits heterogeneous patterns of birefringence and relatively homogeneous, low depolarization. **(C2 and C3)** Fibrous regions covering the lipid-pools of FF generally present with high birefringence. The Lipid-rich areas cause pronounced depolarization. **(D2 and D3)** Calcifications in FC show rather low birefringence and moderate depolarization. Depolarization of calcifications increases with the presence of lipid. **(E2 and E3)** Fibrous caps of ThCFA exhibit heterogeneous birefringence. **(F2 and F3)** Fibrous caps of TCFA typically reveal low birefringence. Depolarization in the diffuse border of the cap promptly transitions from low to high. **(G2 and G3)** The caps of PR have low birefringence. The most intimal layer from 3 to 9 o'clock in the intensity image displays relatively high and heterogeneous birefringence compared to the fragments of white thrombus at 1 and 11 o'clock. White bar = 1 mm. FC = fibro-calcified plaque, FF = fibro-fatty plaque, FP = fibrous plaque, PR = plaque rupture, PS-OFDI = polarization-sensitive optical frequency domain imaging, TCFA = thin cap fibroatheroma, and ThCFA = thick cap fibroatheroma.

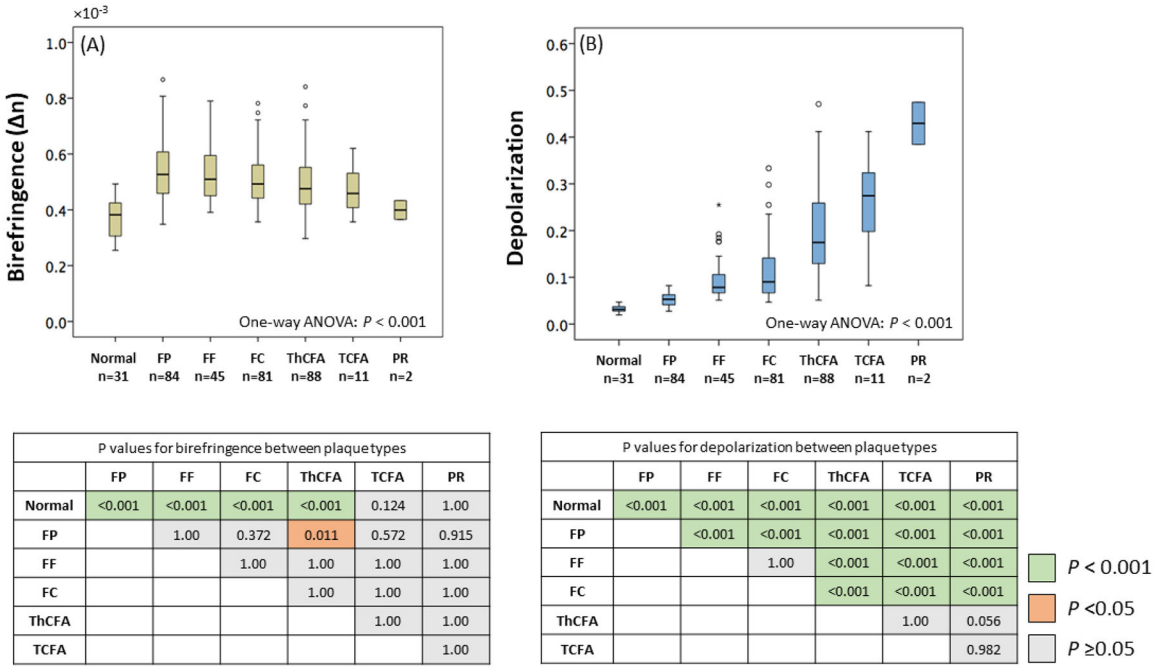

P values for birefringence between plaque types

	FP	FF	FC	ThCFA	TCFA	PR
Normal	<0.001	<0.001	<0.001	<0.001	0.124	1.00
FP		1.00	0.372	0.011	0.572	0.915
FF			1.00	1.00	1.00	1.00
FC				1.00	1.00	1.00
ThCFA					1.00	1.00
TCFA						1.00

P values for depolarization between plaque types

	FP	FF	FC	ThCFA	TCFA	PR
Normal	<0.001	<0.001	<0.001	<0.001	<0.001	<0.001
FP		<0.001	<0.001	<0.001	<0.001	<0.001
FF			1.00	<0.001	<0.001	<0.001
FC				<0.001	<0.001	<0.001
ThCFA					1.00	0.056
TCFA						0.982

Figure 3. Plaque characterization and polarization properties

(A and B) Significant differences in median birefringence and depolarization were observed among the 7 plaque types ($p < 0.001$ for both, One-way ANOVA). **(A)** FPs featured the highest birefringence, followed by FFs, FCs, ThCFAs, TCFAs and PRs in decreasing order, but without statistical significance between most categories. **(B)** A significant gradual variation in depolarization was observed among plaque types ($p < 0.001$, $p < 0.05$ for FP versus FF, ThCFA versus TCFA, TCFA versus PR) except for normal artery versus FP and FF versus FC. Normal indicates normal artery and other abbreviations as in Figure 2.

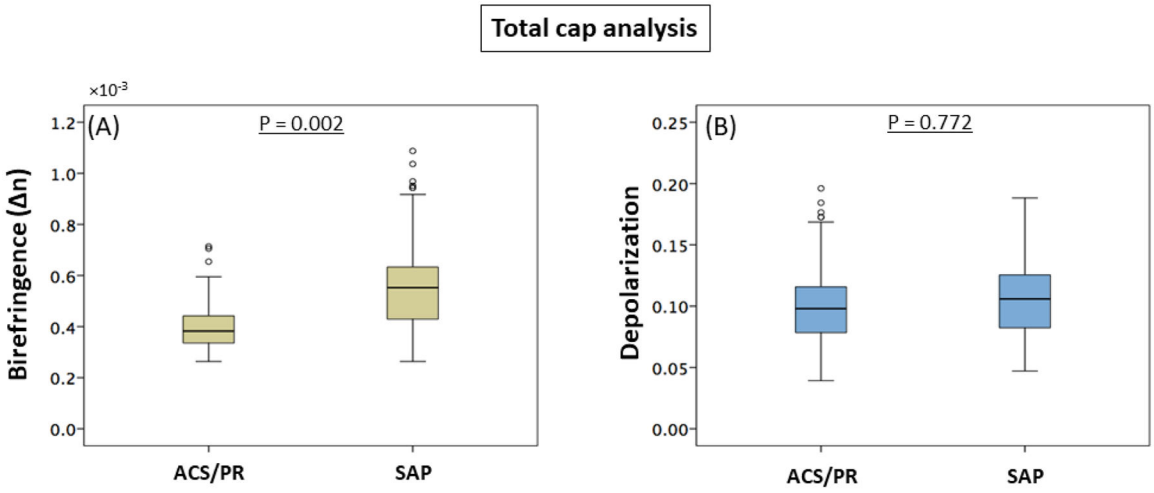

Figure 4. Polarization properties in caps of culprit/target lesions

(A and B) Difference in birefringence **(A)** and depolarization **(B)** between patients with ACS/PR (88 cross-sections from 5 culprit lesions) and SAP (156 cross-sections from 8 target lesions). Fibrous caps in ACS/PR patients exhibited significantly lower birefringence compared to SAP patients. ACS = acute coronary syndrome, PR = plaque rupture, and SAP = stable angina pectoris.

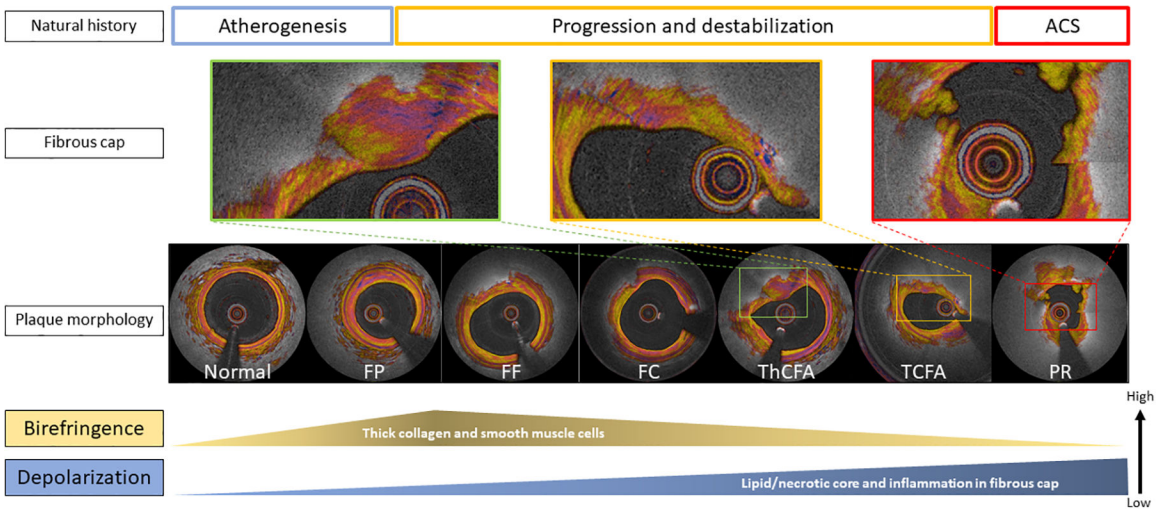

Central illustration. Polarization properties in plaque progression and destabilization

In a less advanced stage of atherogenesis, birefringence and depolarization increase along with the proliferation of thick collagen, smooth muscle cells and lipid content (**atherogenesis and progression**). Birefringence of the plaques declines in hand with the reduction of interstitial collagen, and the development of the lipid/necrotic core, which in turn leads to a significant increase in depolarization, corresponding to the transition of pathological intimal thickening (FP and FF) to a fibroatheroma (**progression and destabilization**). Abbreviations as in Figure 2 and 4.

Table 1.

Patient and OFDI lesion characteristics

	Overall (n = 30)
Patient characteristics	
Age, years	63 ± 9
Male	24 (80)
Hypertension	12 (40)
Diabetes Mellitus	5 (17)
Dyslipidemia	13 (43)
STEMI	1 (3.3)
NSTEMI	5 (17)
Unstable angina	6 (20)
Previous myocardial infarction	8 (27)
Previous PCI	14 (47)
Previous CABG	4 (13)
Imaged vessel (n=36)	
LAD	18 (50)
LCX	6 (17)
RCA	12 (33)
OFDI lesion characteristics (n = 342)	
Analyzed frames	342
Luminal area, mm^2	6.1 ± 3.3
Percent area stenosis, %	40 ± 20
Plaque morphology	
AIT	31 (9.1)
FP	84 (25)
FF	45 (13)
FC	81 (24)
ThCFA	88 (26)
TCFA	11 (3.2)
PR	2 (0.6)
Lipid arc, degree	57 ± 72
Calcium arc, degree	73 ± 50
Minimum fibrous cap thickness, μm	140 ± 81
Polarization properties	
Birefringence, $\times 10^{-3}$	0.50 ± 0.11
Depolarization	0.12 ± 0.09

Variables are expressed as mean ± SD or n, (%). ACS = acute coronary syndrome, AIT = adaptive intimal thickening, CABG = coronary artery bypass graft, CAD = coronary artery disease, FC = fibro-calcified plaque, FF = fibro-fatty plaque, FP = fibrous plaque, PCI = percutaneous coronary intervention, LAD = left anterior descending coronary artery, LCX = left circumflex coronary artery, NSTEMI = non- ST-segment elevation myocardial infarction, PCI = percutaneous coronary intervention, PR = plaque rupture, RCA = right coronary artery, SAP = stable angina

pectoris, STEMI = ST-segment elevation myocardial infarction, TCFA = thin cap fibroatheroma, ThCFA = thick cap fibroatheroma, and OFDI = optical frequency domain imaging.

Table 2.

OFDI and polarimetry lesion characteristics in culprit/target lesion

	ACS/PR group (n = 5)	SAP group (n = 8)	P-value
Analyzed frames	88	156	
OFDI lesion characteristics			
Luminal area, mm^2	3.7 ± 2.1	3.8 ± 2.2	0.871
Percent area stenosis, %	56 ± 23	55 ± 22	0.934
Lipid arc, degree	219 ± 88	171 ± 72	0.045
Calcium arc, degree	95 ± 36	100 ± 62	0.951
Minimum fibrous cap thickness, μm	219± 109	291± 146	0.027
Mean fibrous cap thickness, μm	377± 124	406± 125	0.506
NSD in total cap	2.0 ± 1.5	2.2 ± 1.6	0.596
NSD in focal cap	4.4 ± 3.2	3.9 ± 3.2	0.533
Polarization properties			
Birefringence (plaque), $\times 10^{-3}$	0.44 ± 0.07	0.52 ± 0.08	0.001
Birefringence (total cap), $\times 10^{-3}$	0.42 ± 0.10	0.53 ± 0.16	0.002
Birefringence (focal cap), $\times 10^{-3}$	0.38 ± 0.10	0.49 ± 0.18	<0.001
Depolarization (plaque)	0.28 ± 0.12	0.21 ± 0.12	0.034
Depolarization (total cap)	0.10 ± 0.04	0.10 ± 0.03	0.772
Depolarization (focal cap)	0.11 ± 0.05	0.11 ± 0.04	0.845

Variables are expressed as mean ± standard deviation. P-values were obtained by generalized liner model using GEE. GEE = generalized estimating equation and NSD = normalized standard deviation. Other abbreviations as in Table 1.

Table 3.

Relationships between polarization properties in total fibrous cap, clinical presentation, and OFDI parameters

	Total cap analysis							
	Birefringence				Depolarization			
			95% CI				95% CI	
	β	P-value	Lower	Upper	β	P-value	Lower	Upper
Age (per 5 years increase)	0.003	0.813	−0.019	0.024	0.001	0.782	−0.007	0.009
ACS/PR	−0.156	0.002	−0.254	−0.058	0.003	0.772	−0.014	0.019
Fibrous cap thickness, mean (per 10 μm increase)	0.002	0.264	−0.001	0.005	−0.001	< 0.001	−0.002	−0.001
Lipid arc (per 10° increase)	−0.004	0.109	−0.008	0.001	0.001	0.001	0.0005	0.0021
Percent area stenosis (per 10% increase)	0.006	0.643	−0.018	0.030	0.001	0.647	−0.002	0.004
Calcium arc (per 10° increase)	0.003	0.339	−0.004	0.011	0.001	0.477	−0.001	0.003
NSD	−0.021	0.013	−0.037	−0.004	0.005	0.062	−0.0002	0.0092

The relationship between polarization properties and clinical and OFDI parameters were determined by unadjusted generalized linear model using a GEE to take into consideration the intra-subject correlations among multiple cross-sectional images from individual patients. β and 95% CI for birefringence are given in units of $\times 10^{-3}$. CI = confidence interval, GEE = generalized estimating equation, and other abbreviations as in Table 1.

Table 4.

Associations of polarization properties in focal fibrous cap and OFDI parameters

	Focal cap analysis							
	Birefringence				Depolarization			
			95% CI				95% CI	
	β	P-value	Lower	Upper	β	P-value	Lower	Upper
ACS/PR	−0.138	< 0.001	−0.211	−0.065	0.002	0.845	−0.022	0.027
Fibrous cap thickness, thinnest (per 10 μm increase)	0.005	0.001	0.002	0.008	−0.001	0.005	−0.0016	−0.0003
NSD	−0.012	0.001	−0.020	−0.005	0.004	< 0.001	0.002	0.006

The relationship between polarization properties and clinical and OFDI parameters were determined by unadjusted generalized linear model using a GEE to take into consideration the intra-subject correlations among multiple cross-sectional images from individual patients. β and 95% CI for birefringence are given in units of $\times 10^{-3}$. Abbreviations as in Table 1 and Table 3.